In Situ Preparation and Properties of High-Solid-Content and Low-Viscosity Poly(methyl methacrylate/*n*-butyl acrylate/acrylic acid)/Poly(styrene/acrylic acid) Composite Latexes

Zhao-Quan Ai,[1,2] Qi-Long Zhou,[2] Chang-Sheng Xie,[1] Hong-Tao Zhang[2]

[1]*Faculty of Material Science and Engineering, Huazhong University of Science and Technology, Wuhan 430074, China*
[2]*Faculty of Chemistry and Material Science, Hubei University, Wuhan 430062, China*

Received 4 September 2005; accepted 3 August 2006
DOI 10.1002/app.25347
Published online in Wiley InterScience (www.interscience.wiley.com).

ABSTRACT: With monodispersed poly(methyl methacrylate/*n*-butyl acrylate/acrylic acid) [P(MMA/BA/AA)] seeded latex with a particle size of 485 nm and a solid content of 50 wt % as a medium, a series of stable P(MMA/BA/AA)/poly(styrene/acrylic acid) composite latexes with a high solid content (70 wt %) and low viscosities (500–1000 mPa · s when the shear rate was 21 s^{-1}) was prepared *in situ* via simple two-step semicontinuous monomer adding technology. The coagulum ratio of polymerization was about 0.05 wt %. The particle size distribution of such latexes was bimodal, in which the large particle was about 589 nm and the small one was about 80 nm. The latexes combined good mechanical properties with good film-forming properties. Differential scanning calorimetry showed that the corresponding latex film had a two-phase structure. The morphology of the latex film was characterized with atomic force microscopy and scanning electron microscopy. © 2006 Wiley Periodicals, Inc. J Appl Polym Sci 103: 1815–1825, 2007

Key words: latices; composites; emulsion polymerization

INTRODUCTION

Increasing the solid content (SC) of polymer latexes, that is, making high-solid-content (HSC) latexes, is of great industrial and theoretical interest recently because this increases the space–time yield of the reactor and makes product transport more efficient and less costly. In addition, a reduction in the water content of waterborne coatings allows a reduction in film formation and drying time, which will be helpful in replacing solvent-borne coatings and meeting the environmental protection demands.[1–3]

The viscosity and coagulum ratio (CR) are two key properties during the preparation of HSC latexes. In other words, the preparation of low-viscosity and low-CR HSC latexes is the goal. Theoretical and experimental studies have indicated that SC, viscosity, and polymer colloid particle size distribution (PSD) are closely related. Farris,[4] Suddth,[5] and Schneider and coworkers[6] once studied their relationship on the bases of predecessor's rheology formulas,[4,5] such as the Einstein equation and Mooney formula, and computer models.[6] They suggested, for the bimodal PSD latexes, that when the large/small particle size ratio was 7–8 and the volume fraction of small particles was 15–20%, in theory, the latexes would have the lowest viscosity at the same SC or the highest SC at the same viscosity. Chu and coworkers,[7,8] Greenwood et al.,[9,10] and Berend and Richtering[11] blended prepared monodispersed latexes of different size and investigated their relationship and obtained the same results.

As a result, the production of latexes with controlled PSDs has become the main approach to the preparation of HSC latexes.[12–17] In a previous work,[18] we prepared a coagulum-free poly(methyl methacrylate/*n*-butyl acrylate/acrylic acid) [P(MMA/BA/AA)] latex with the SC on the order of 72 wt % and with a viscosity of 400 mPa s (shear rate = 21 s^{-1}) via a technology that used seeded latexes with large particle sizes as a medium to replace water. Compared to other methods, such technology lowered the emulsifier dosage (2 wt % of monomer), simplified the preparation process, and shortened the production period.

A major problem associated with waterborne coatings arises from the competition between film formation and film mechanical properties. For instance, low glass-transition-temperature (T_g) polymer latexes have good film-forming abilities, but the corresponding films exhibit low Young's moduli. However, polymer latex blends are expected to compromise these two aspects, especially blends of hard and soft latex particles. In addition, latex blending is an attractive strategy for the development of new durable coatings with zero volatile organic compounds. It has been envisioned that the soft latex particles (i.e., polymers with low

Correspondence to: Z.-Q. Ai (aiz-q@sohu.com).

Journal of Applied Polymer Science, Vol. 103, 1815–1825 (2007)

TABLE I
Recipes and Characteristics of the Seeded Latexes

Latex		BA (g)	MMA (g)	AA (g)	H_2O (g)	OS-15 (g)	SDS (g)	APS (g)	SHC (g)	T (°C)	Time (min)	CR (%)	D_p (nm)
SE	IC	24	16	—	360	1.4	0.02	0.72	0.24	75	50	0.06	485
	EM	269	179	12.4	128	10	0.12	0.72	—	75	300		

SE = seeded latex; IC = initial charge; EM = emulsified monomers; Time = reaction and feeding times; D_f = particle size of seeded intexes; T = temperature during the initial and feeding periods. The temperature was increased to 80°C after the addition for another 30 min to finish the reaction.

T_g's) will deform and form a continuous film with the embedded hard latex particles (high T_g), whose presence will impart desirable mechanical or optical properties.[19–21]

Undoubtedly, HSC latex has such trouble, too, which has always been omitted in the preparation of HSC latexes. To the best of our knowledge, on the other hand, most of the academic researches involving latex blends have been done on the basis of the blending of hard and soft latex particles at the same size[22,23] and have not been aimed at the preparation of HSC latexes (in fact, one cannot obtain HSC latexes with SCs above 70% and low viscosity, theoretically due to the ratio of particle sizes mentioned previously). Even when HSC latexes are prepared via the blending of latexes with different size, a condensing step is needed at last, which limits its industrial applications. Actually, few studies have focused on the synthesis of HSC latexes with different polymer components, not to mention the compatibility of different polymers in such a system.

In this study, a series of stable HSC P(MMA/BA/AA)/poly(styrene/acrylic acid) [P(St/AA)] composite latexes were prepared *in situ* with a seeded P(MMA/BA/AA) latex with large size as a medium with the addition of two monomer feeding steps. The basic idea of such a technology is to design the hardness of colloid particles on the basis of the control of PSD and to obtain HSC latexes with not only the features of HSC and low viscosity but also a combination of good film-forming and film mechanical properties. The morphologies of the colloid particles, the rheological properties and film-forming properties of the latex, and the phase structure and mechanical properties of the latex film were characterized.

EXPERIMENTAL

Materials

Butyl acrylate (BA), methyl methacrylate (MMA), styrene (St), and acrylic acid (AA; Beijing Dongfang Chemical Co., Beijing, China) monomers were filtered through inhibitor removal columns before use. Ammonium persulfate (APS) and sodium hydrocarbonate (SHC; Tianjin Reagent Manufacturer No. 6, Tianjin, China) and aliphatic alcohol polyoxyethylene ether (OS-15) and sodium dodecyl sulfonate (SDS; Beijing Qiuxian Chemical Manufacturer, Beijing, China) were all used as received. The water was deionized.

Latex synthesis

All syntheses were performed in a 1000-mL, four-necked flask equipped with a reflux condenser, a nitrogen gas inlet tube, a polytetrafluroethylene (PTFE) stirrer, a feed tube for monomers or preemulsified monomers, and a thermometer. Preemulsified monomer was prepared in a mononeck flask by the addition of water, emulsifier, buffer, and monomers successively under vigorous stirring at room temperature with the recipe shown in Table I.

Large-size seeded latex

Large-size seeded latex was prepared with seeded semicontinuous emulsion polymerization, which was improved in ref. 15, and the recipe and properties are listed in Table I. First, a small-size seeded latex with a SC of 10 wt % was prepared with the initially charged materials at 75°C, and then, the emulsified monomer was added over 300 min at the same temperature. After the addition was finished, the temperature was raised to 80°C and kept there for another 30 min to complete the polymerization.

HSC P(MMA/BA/AA)/P(St/AA) composite latexes

The previously prepared large-size seeded latex, SDS, APS, and SHC were mixed in the reactor; then, the temperature was raised to 80°C, and the reaction was started. At the same time, a two-step monomer addition was begun. In the first step, MMA/BA/AA with the same components as the seeded latex monomer was added. After the first addition completed, the temperature was kept at 80°C for 30 min. Then, the second monomer (i.e., St/AA) addition was begun. The total monomer feeding time was about 120 min, excluding the temperature-keeping period. After the addition of all monomers, the polymerization was conducted for another 40 min to complete the reaction. All the recipes are tabulated in Table II.

TABLE II
Formation and Characteristics of HSC Latexes

Latex		SE (g)	BA (g)	MMA (g)	AA (g)	St (g)	APS (g)	SHC (g)	SDS (g)	Time (min)	SC (%)	CR (%)	SS
HNCE	IC	500	45	30	2.10		1.05	0.90	10	20	70	<0.05	A
	AM	—	138	92	6.44	—	—	—	—	120			
HCE1	IC	500	45	30	2.10		0.90	0.90	10	20	70	<0.05	A
	AM1	—	105	70	4.90	—	—	—	—	90			
	AM2	—	—	—	1.54	55	0.15	—	—	30			
HCE2	IC	500	45	30	2.10	—	0.90	0.90	10	20	70	<0.05	A
	AM1	—	75	50	3.50	—	—	—	—	60			
	AM2	—	—	—	2.94	105	0.15	—	—	60			
HCE3	IC	500	45	30	2.10	—	0.90	0.90	10	20	70	<0.05	A
	AM1	—	57	38	2.66	—	—	—	—	45			
	AM2	—	—	—	3.78	135	0.15	—	—	75			
HCE4	IC	500	45	30	2.10	—	0.90	0.90	10	20	70	0.38	A
	AM1	—	42	28	1.96	—	—	—	—	30			
	AM2	—	—	—	4.48	160	0.15	—	—	90			
HCE5	IC	500	45	30	2.10	—	0.90	0.90	10	20	—	—	—
	AM1	—	24	16	1.12	—	—	—	—	150			
	AM2	—	—	—	5.32	190	0.15	—	—	—			

SE = the seeded latex prepared with the recipe in Table 1; IC = initial charge; AM = additional monomers; HNCE = HSC noncomposite latexes; HCE = HSC composite latexes. AM2 was added 30 min after the addition of AM1. The temperature during the initial and feeding periods was 80°C; the temperature was raised to 85°C for another 40 min after the addition to finish the reaction.

HSC (70 wt %) P(MMA/BA/AA) noncomposite latex

For comparison, a HSC (70 wt %) noncomposite P(MMA/BA/AA) latex, which had same monomer component as the seeded latex and the first-feeding monomers of the composite latexes, was prepared with similar technology (i.e., HNCE in Table II). The only difference between them was that the monomer of the latter was added continuously in one step.

Preparation of latex film

For the films used for mechanical tests and scanning electron microscopy (SEM), diluted latex with a SC of 50% was used, and the latexes were dried under controlled conditions (temperature = 24 ± 2°C; relative humidity = 60 ± 5%) on PTFE films for 20 days. The thickness of these films was about 1.5 ± 0.05 mm. For the films used for atomic force microscopy (AFM), one drop of diluted latex with a SC of 10% was cast on a microscope round cover glass with a diameter of 13 mm and a thickness of 0.13–0.17 mm (Mingzhu Industrial Instrument Glass Factory, Ningbo, Zhejiang Province, China) under the same conditions for 10 days. The thickness of the dried films was around 15 μm.

Measurement

Samples were withdrawn during the process, and the polymerization was stopped with hydroquinone. The overall conversion was determined gravimetrically. SC was measured with thermogravimetry. The particle size and distribution of seeded latex were characterized with an Autosizer Loc-FC-963 apparatus (Malvern Instruments, Malvern, UK) and checked with transmission electron microscopy (TEM; JEM-100SX, Jeol, Tokyo, Japan), which indicated that the seeded latex was monodispersed and the particle size was 485 nm, as shown in Figure 1. The particle size of the HSC latexes were measured with a statistical method with TEM, that is, with an average size of 200 colloid particles as the particle size. The rheological properties of the latexes were estimated with a rotation viscometer (NXS-11, Chengdu Instruments Co., Chendu, China) at room temperature. Differential scanning calorimetry (DSC) experiments were performed on a PerkinElmer (Wellesley, MA) Pris 1 differential scanning calorimeter in a N_2 atmosphere at a

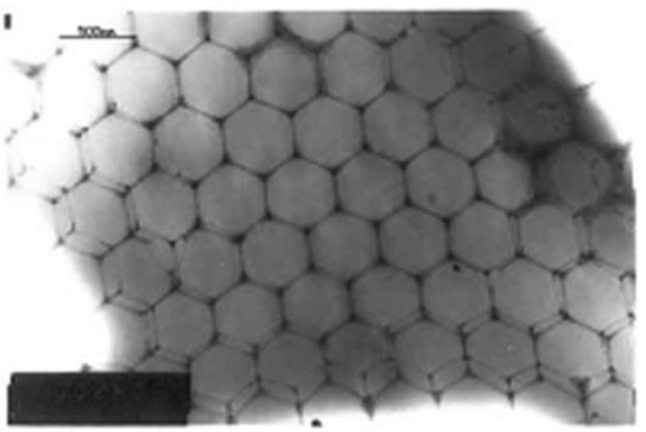

Figure 1 TEM micrographs of the monodispersed seeded latex.

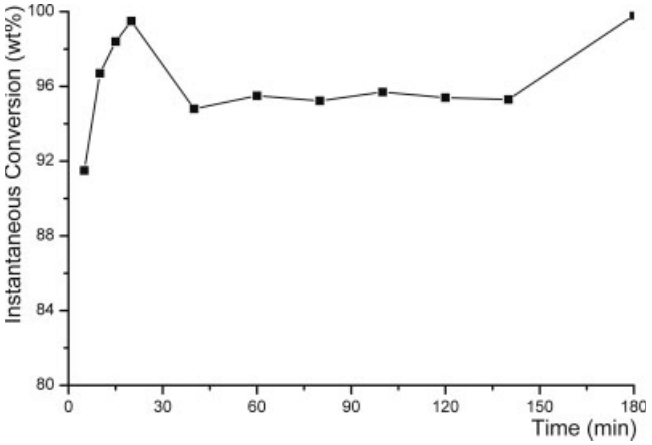

Figure 2 Instantaneous conversion of HNCE during the polymerization as a function of time. Time counting began when the temperature rose to 80°C.

rate of 20°C/min, and the samples were prepared by the drying of the film used for mechanical tests in an oven at 105°C for 1 night. The latex films were cut into dumbbell-shaped specimens according to National Standard GB/1040-92 (China), and tensile tests were carried out with an AG-10KNA universal testing machine (Shimadzu, Kyoto, Japan) with a crosshead speed at 200 mm/min. At least five specimens were tested. The morphological features of the films were analyzed with AFM (Nanoscope IIIa, Digital Instruments, Buffalo, NY) with tapping mode at room temperature in air and with SEM (FEI SIRION200, Philips Co., Hillsboro, OR). The stability during polymerization was evaluated with CR, which was determined as follows. The latexes were filtered through a 120-mesh filter at ambient temperature. Then, the coagulum in the filter and that on the stirrer and the wall of reactor was collected carefully. The coagulum was rinsed with deionized water and dried in an oven at 105°C for 1 night. CR was calculated as follows:

$$\mathrm{CR}\ (\%) = G_2/(G_1 - G_0) \times 100 \qquad (1)$$

where G_1 is the mass of the latex, G_2 is the mass of the dried coagulum, and G_0 is the mass of the volatile materials in the latex.

Storage stability (SS) of the latex was estimated according to the state of the latexes after storage for a month at ambient temperature, where AA is excellent, A is good, B is fair, C is little precipitate and easy to redisperse, and D is little precipitate and dispersible.

TABLE III
Particle Sizes of Large and Small Colloid Particles in the HSC Latexes in Table II

	HNCE	HCE1	HCE2	HCE3	HCE4
Large particle size (nm)	592	589	597	583	582
Small particle size (nm)	80	78	80	82	81

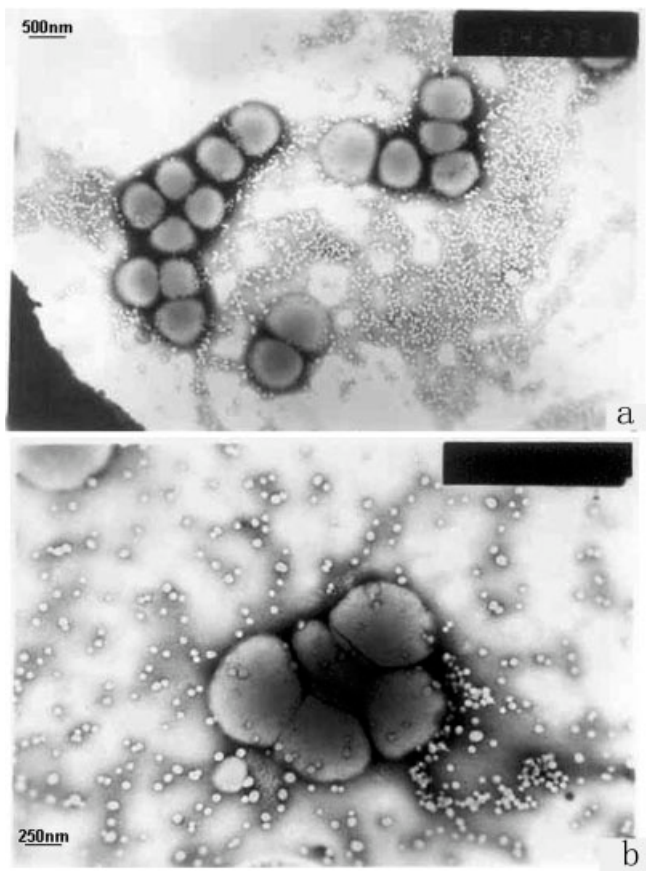

Figure 3 TEM micrographs of HSC composite latexes (a) HCE3 and (b) HCE4 prepared as shown in Table II. Phosphotungstic acid was used as a marker (observed at room temperature).

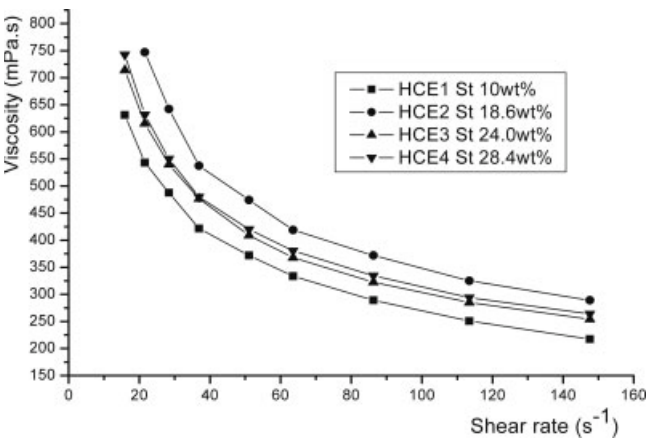

Figure 4 Viscosity of the HSC P(MMA/BA/AA)/P(St/AA) composite latexes shown in Table II as a function of shear rate.

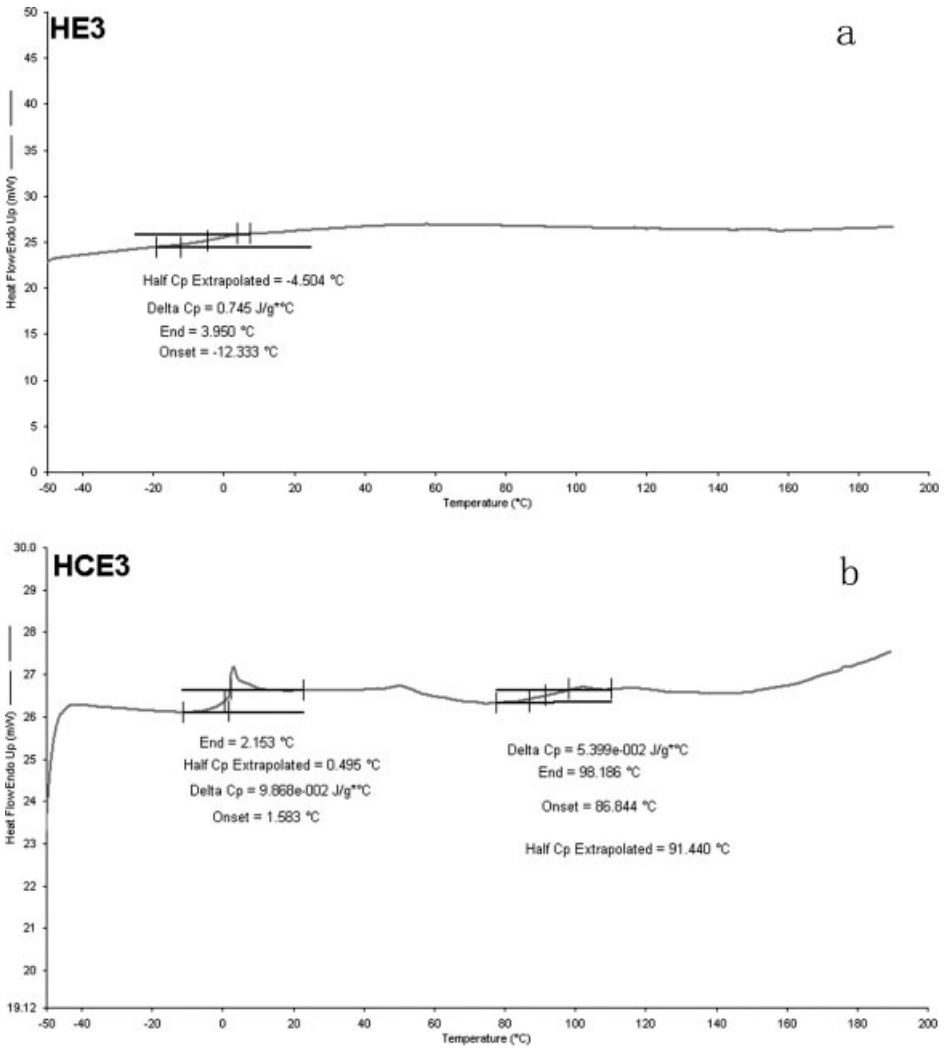

Figure 5 DSC thermograms of the noncomposite and composite latexes (a) HNCE and (b) HCE3 shown in Table II (at a heating rate of 20°C/min from −50 to 200°C). Cp = capacity of heat.

RESULT AND DISCUSSION

Analysis of the polymerization course

Figure 2 shows the polymerization rate of HNCE in Table II; the monomer was in a so-called hungry state during the course of reaction. So were HCE1–HCE4 during the first monomer feeding stage at the same monomer feeding rate (ca. 2.0 g/min). This indicates that the residual acrylate monomer could be neglected when the second monomer adding step began; the reaction continued for 30 min more after the completion of the first monomer adding step. As a result, the St added during the second monomer adding step polymerized mainly in two sites. One was the newly nucleated P(St/AA) colloid particles, which formed the new hard (with high T_g) small particles. The other was the surface of the existing P(MMA/BA/AA) colloid particles, which formed P(MMA/BA/AA)-*cs*-P(St/AA) colloid particles. The larger the amount of St and emulsifier was used, the greater the number of hard small particles and core–shell colloid particles were. In addition, when one considers the specific monomer adding sequence and the fact that

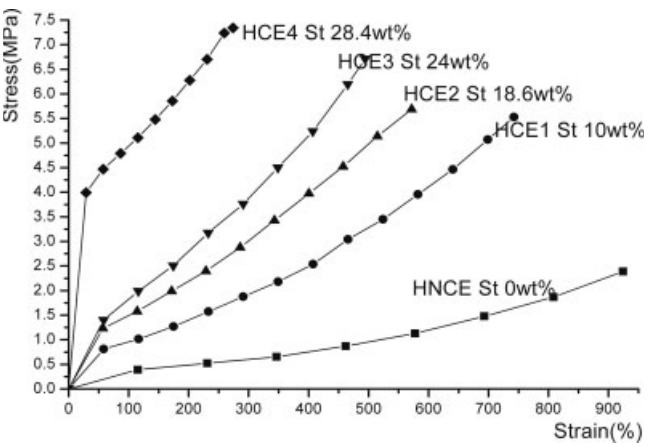

Figure 6 Stress–strain curves of HSC P(MMA/BA/AA)/P(St/AA) latex films differing in their weight fractions of St.

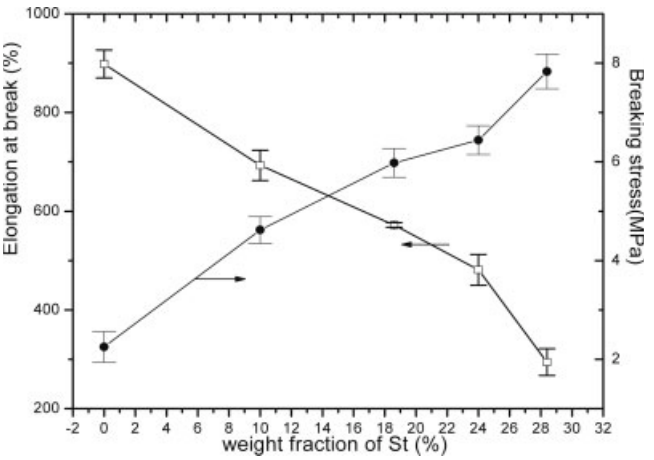

Figure 7 Elongation at break and breaking stress versus the weight fraction of St of the HSC composite P(MMA/BA/AA)/P(St/AA) latex film.

acrylate monomers had polymerized completely when the St adding stage began, one can envision that some St monomer polymerized with the residual free radical on the acrylate polymer, and thus, some block (or graft) polymer came into being. Certainly, one could not produce block (or graft) polymer with this method qualitatively or quantitatively. However, the inevitable block (or graft) polymer in this system, even in a small amount, would improve the compatibility and phase structure of the corresponding latex film. This is one of the advantages of composite latexes prepared *in situ*, compared to conventional blend latexes.

CR during the polymerization

As shown in Table II, HCE5 agglomerated completely during the second monomer adding step; CRs of HCE1–HCE3 were all below 0.05%, and CR of HCE4 was 0.38%. Obviously, when the content of St was below 30 wt %, the polymerization course was relatively stable, especially when it was below 25 wt %. When it exceeded 30 wt %, the latex polymerization could not be performed normally under such conditions.

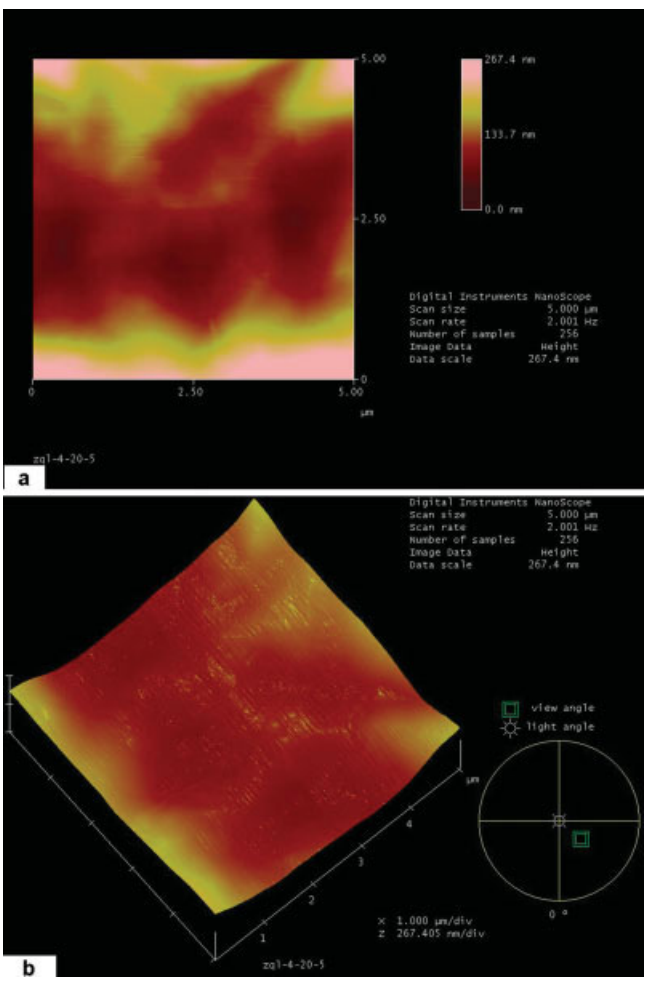

Figure 8 AFM images of the HNCE film (0 wt % St): (a) top view, 5 × 5 μm, and (b) three-dimensional view, 5 × 5 μm. [Color figure can be viewed in the online issue, which is available at www.interscience.wiley.com.]

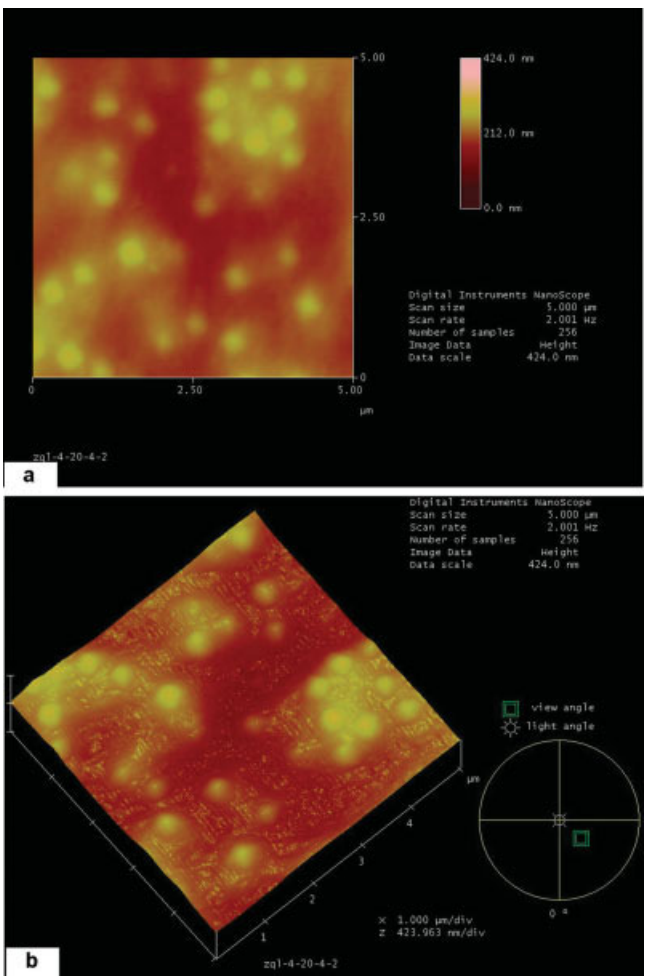

Figure 9 AFM images of the HCE2 film (10.0 wt % St): (a) top view, 5 × 5 μm, and (b) three-dimensional view, 5 × 5 μm. [Color figure can be viewed in the online issue, which is available at www.interscience.wiley.com.]

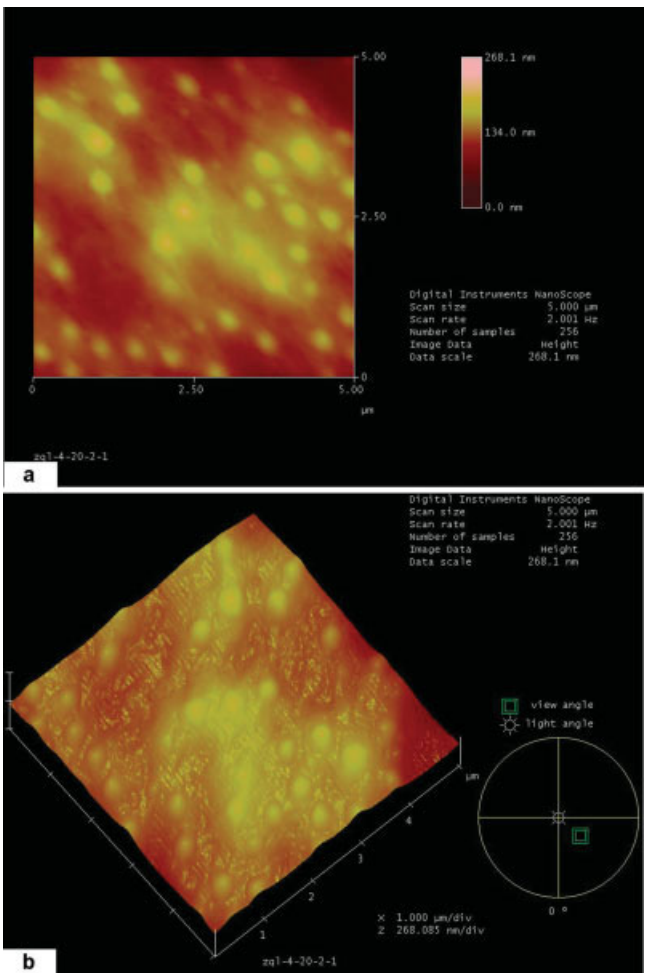

Figure 10 AFM images of the HCE2 film (18.6 wt % St): (a) top view, 5 × 5 µm, and (b) three-dimensional view, 5 × 5 µm. [Color figure can be viewed in the online issue, which is available at www.interscience.wiley.com.]

Properties of the latexes

Particle size and distribution

Figure 3 shows the TEM pictures of the HSC composite latexes, showing that the distribution of composite latexes particles was bimodal. In addition, the particle size of the HSC noncomposite and composite latexes are shown in Table III, which shows that the large particle was about 589 nm and the small one was about 80 nm and the ratio of the large and small particle sizes was about 7.4. In other words, addition of St had little effect on the size and distribution of the polymer colloid particles in this system.

Rheology properties of the composite latexes

From the rheograms of the composite latexes (Fig. 4), one can see that the composite latexes were a pseudoplastic fluid and that their viscosity was relatively low (<650 mPa s at 28.38 s^{-1}). This was possibly due to the bimodal distribution of particles and the appropriate size ratio.[10] The viscosity of the composite latexes was much higher than the noncomposite latex with a similar SC (HNCE in Table II; 185 mPa s at 28.38 s^{-1}). An increase in particle hardness, which is disadvantageous to the pack and deformation of particles, was one of the possible reasons. However, the viscosity appeared to have no linear relationship with the weight fraction of St. When the content of St was 19 wt % (HCE2), the latex had the highest viscosity in the studied range, and the difference of the content of St between HCE3 and HCE4 had no embodiment in viscosity.

Film-forming properties of the latexes

Film-forming properties of composite latexes are described with criteria based on the maximum weight fraction of hard latex particles (φ_{max}), which allows good film formation under controlled drying conditions.[23] Films of noncomposite and composite latexes were obtained by drying of the corresponding latexes under controlled conditions (temperature = 24 ± 2°C,

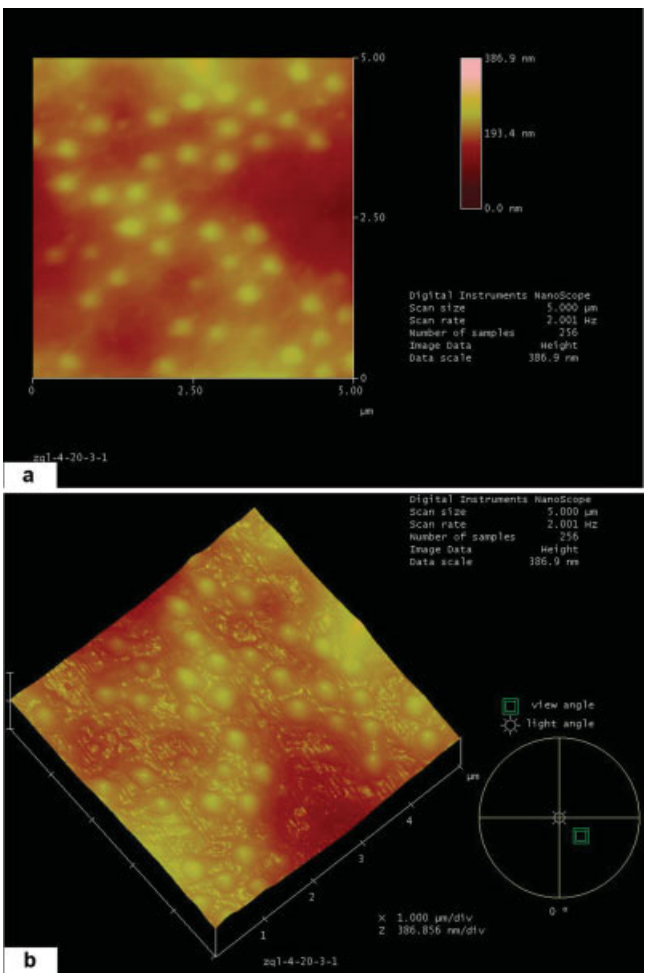

Figure 11 AFM images of the HCE3 film (24.0 wt % St): (a) top view, 5 × 5 µm, and (b) three-dimensional view, 5 × 5 µm. [Color figure can be viewed in the online issue, which is available at www.interscience.wiley.com.]

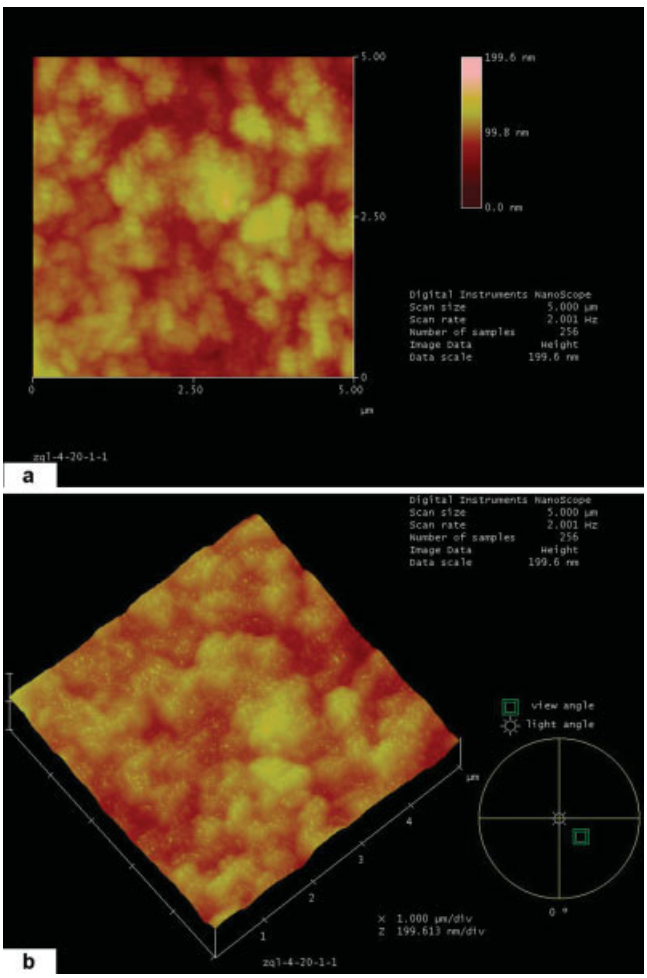

Figure 12 AFM images of the HCE3 film (28.4 wt % St): (a) top view, 5 × 5 µm, and (b) three-dimensional view, 5 × 5 µm. [Color figure can be viewed in the online issue, which is available at www.interscience.wiley.com.]

relative humidity = 60 ± 5%) onto the PTFE plates. Under such conditions, HNCE and HCE1–HCE3 could form good films; that is, the content of hard particles was below φ_{max}, and the latex had good film-forming properties. HCE4, however, had local cracks, which meant the hard particle content approached φ_{max} in this system. It is a pity that a composite latex with a content of St above 30 wt % was not obtained so far, along with the amount of hard particles. As a result, we could not determine φ_{max} in this system.

SS of the latexes

As shown by the SS column in Table II, HSC noncomposite and composite latexes all had good SS.

Properties of the latex films

T_g values of the latex films

Figure 5 shows the DSC curves of the polymers of HNCE and HCE3 shown in Table II. Obviously, the noncomposite latex (HNCE) had only one T_g (−4.5°C), and the composite latex (HCE3) had two T_g's (0.5 and 91.4°C), with the low T_g attributed to the P(MMA/BA/AA) phase and the high one attributed to the P(St/AA) phase. The T_g value of P(MMA/BA/AA) in the composite latex changed from −5 to 0.5°C. This shift was possibly due to the existence of some block (or graft) copolymer P(MMA/BA/AA)-*b*-P(St/AA), as analyzed previously, which could have improved the compatibility of the two phases.

Mechanical behavior of the latex films

Figure 6 presents stress–strain curves of composite latexes with different weight fractions of St. As expected, an increase in the weight fraction of St enhanced the stiffness of the latex films. The influence of the weight fraction of St on the elongation at break and breaking stress is presented in Figure 7. In the

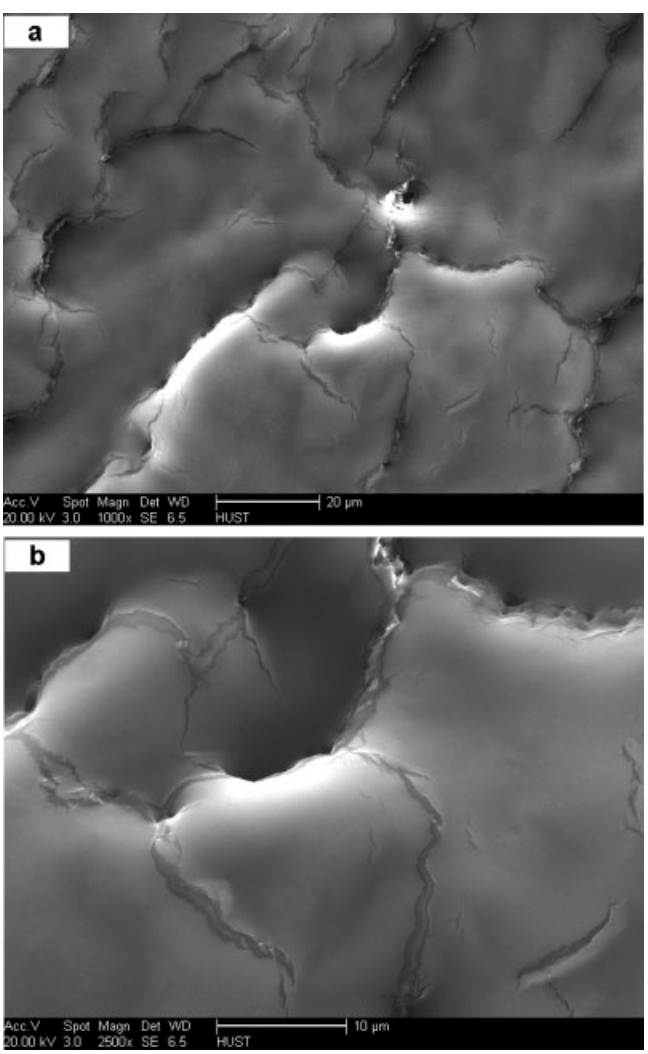

Figure 13 SEM micrographs of the HSC P(MMA/BA/AA) latex films (HNCE in Table II): (a) 1000 and (b) 2500×.

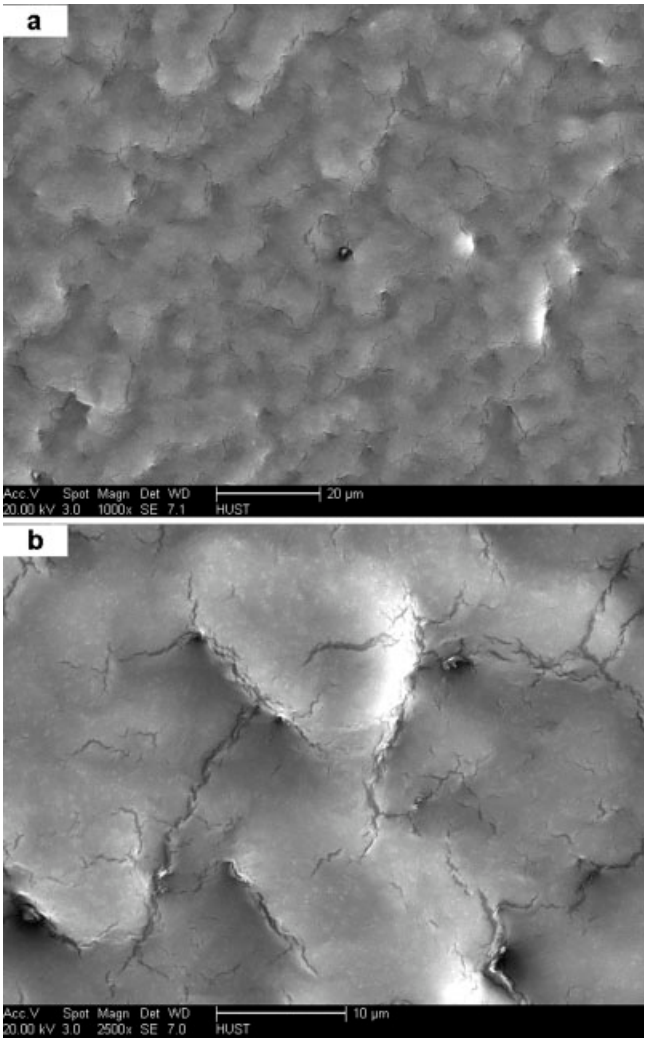

Figure 14 SEM micrographs of the HSC composite latex film [P(MMA/BA/AA)/P(St/AA)] with St = 10.0 wt % (HCE1 in Table II): (a) 1000 and (b) 2500×.

studied range, as the content of St increased, the elongation at break decreased, and the tensile strength increased remarkably. The former changed from 898% (0 wt % St) to 481% (24.0 wt % St) and 294% (28.4 wt % St). The latter changed from 2.3 MPa (0 wt % St) to 6.4 MPa (24.0 wt % St) and was even 7.8 MPa when the weight fraction of St was 28.4 wt %. The result, plus their good film-forming properties, supported the basic idea of our design of such HSC composite latexes.

Surface morphological structure of the composite latex films

Figures 8–12 present the AFM pictures of noncomposite and composite latex films differing in their weight fraction of St. As shown, the noncomposite P(MMA/BA/AA) latex formed an integral film and left no colloid particles under such condition; P(MMA/BA/AA)/P(St/AA) composite latex film, however, contained some residual particles, the amount of which increased with the weight fraction of St. When the St fraction was 28.4 wt % (HCE4), a lot of particles aggregated together to form a honeycomb structure (Fig. 12), which indicated that the film could not be formed in a microscope under such conditions. Such results favored the foregoing phenomenon that the corresponding composite latex film had local cracking. The residual particles mainly consisted of large particles (ca. 550 nm), including some small ones (ca. 80 nm). In addition, the surface of these particles was smooth, excluding the possibility of the new-forming hard particles aggregating onto the surface of large particles due to instability. Also, such large (ca. 550 nm) P(St/AA) colloid particles could not be formed under such conditions. As a result, such residual particles may have had a core–shell structure, the core of which mainly consisted of P(MMA/BA/AA) and the shell of which consisted of

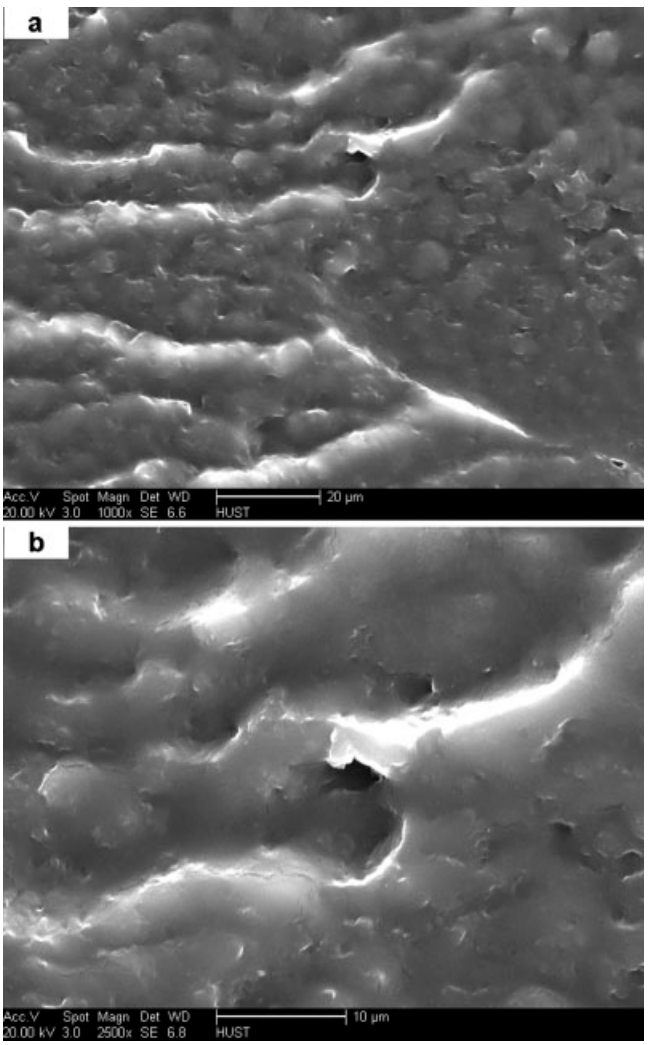

Figure 15 SEM micrographs of the HSC composite latex film [P(MMA/BA/AA)/P(St/AA)] with St = 18.6 wt % (HCE2 in Table II): (a) 1000 and (b) 2500×.

P(St/AA). That is, the core was soft, and the shell was hard. Undoubtedly, such a structure was disadvantageous to the film formation of composite latexes because the corresponding particles could not deform at room temperature. As to the new-forming P(St/AA) particles, they could not deform during the film-forming course at all and were embodied in the matrix of the P(MMA/BA/AA) film. In conclusion, the addition of St affected the film-forming properties of latex to some extent. If one considers the mechanical properties of the latex films, the appropriate content of St is a key issue in the preparation of good-performance composite latexes. Exactly 24 wt % St was the best choice.

The influence of the weight fraction of St on the film morphology was also clearly revealed by the morphologies of the fracture surface. Figures 13–17 show the micrographs of the fractured surfaces obtained by SEM. It is clear from Figures 13–17 that the greater the amount of St was, the coarser the fractured surface was. Figures 12–16 also show that the fractured surface morphologies underwent two leaps as the fraction of St increased. One appeared when St increased from 10 to 18.6 wt % (Figs. 14 and 15); the surface suddenly became coarse. The other one appeared when the amount changed from 24.0 to 28.4 wt %, and the coarseness increased remarkably.

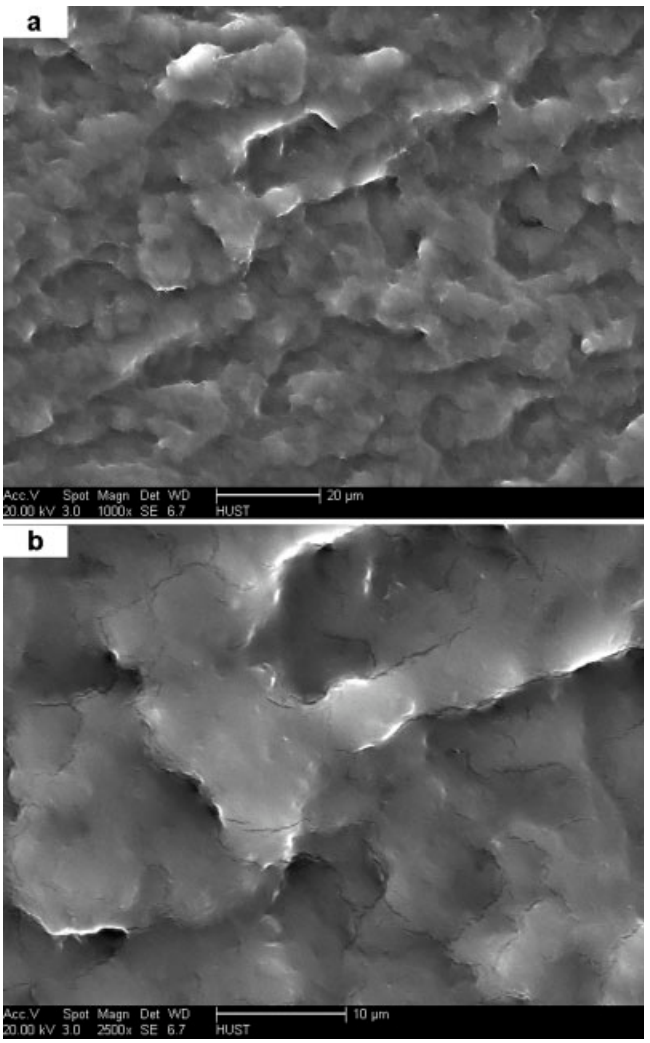

Figure 16 SEM micrographs of the HSC composite latex film [P(MMA/BA/AA)/P(St/AA)] with St = 24.0 wt % (HCE3 in Table II): (a) 1000 and (b) 2500×.

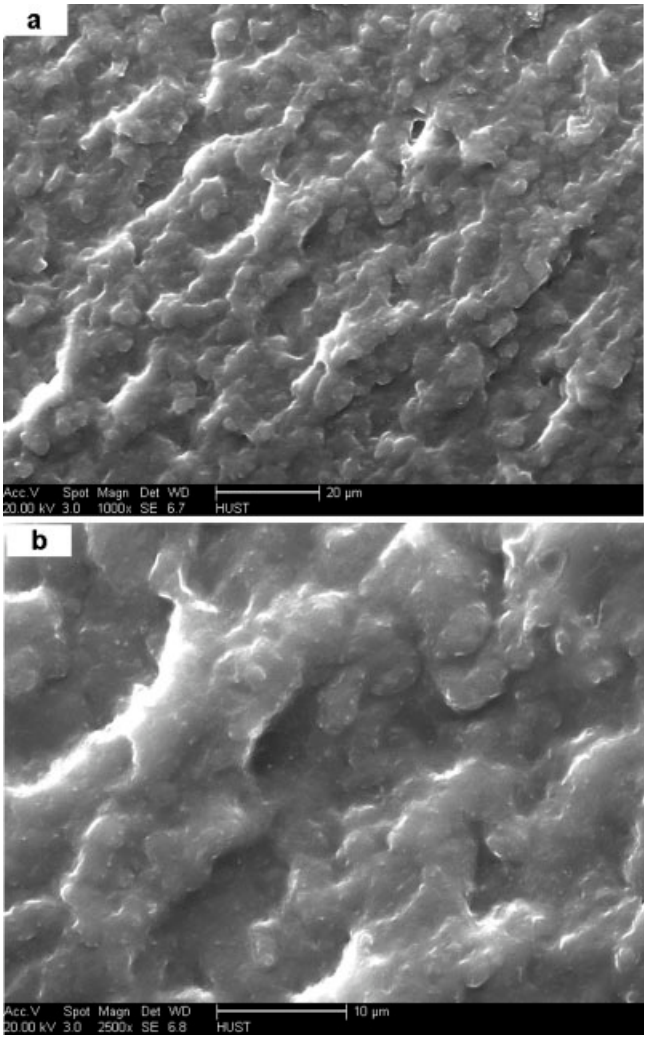

Figure 17 SEM micrographs of the HSC composite latex film [P(MMA/BA/AA)/P(St/AA)] with St = 28.4.0 wt % (HCE4 in Table II): (a) 1000 and (b) 2500×.

CONCLUSIONS

HSC P(MMA/BA/AA)/P(St/AA) composite latexes were prepared at a neglectable coagulum rate (<0.05 wt %), with a large-size monodispersed seeded latex as a medium plus a simple two-step semicontinuous monomer adding technology. With appropriate particle size and distribution, such composite latexes had the features of HSC (70 wt %) and low viscosity (500–1000 mPa · s at 21 s^{-1}); they had good SS. Additionally, DSC, AFM, and TEM indicated that the corresponding latex film

had a two-phase structure, that is, P(MMA/BA/AA) with a T_g of 0.5°C and P(St/AA) with a T_g of 91.4°C. At room temperature, the colloid particles consisting of P(MMA/BA/AA), that is, soft particles, formed an integral film; the particles consisting of P(St/AA), that is, hard particles, and those covered with P(St/AA) were embodied in the film after the film-forming process was completed. Such specific structure combines good film-forming properties of latexes with the high mechanical performance of the corresponding latex films. The results also indicate that as the weight fraction of St increased, the mechanical properties improved, but the film-forming properties decreased. When the weight fraction of St was 24 wt %, the properties of the latex were the best. The tensile strength of the corresponding latex film was 6.4 MPa, compared to 2.3 MPa for noncomposite one; at the same time, it could form an integral film at room temperature.

This work was financially supported by the Natural Science Foundation of Hubei province, China.

References

1. Ai, Z.; Liao, S.; Li, J. Chin Synth Resin Plast 1996, 19, 331.
2. Ai, Z.; Zhou, Q.; Zhang, H. Chin Polym Bull 2004, 3, 43.
3. Guyot, A.; Chu, F.; Schneider, M.; Graillat, C.; McKenna, T. F. Prog Polym Sci 2002, 27, 1573.
4. Farris, R. J Trans Soc Rheol 1968, 12, 281.
5. Suddth, R. D. J Appl Polym Sci 1993, 50, 123.
6. Guyot, A.; Chu, F.; Schneider, M.; Schneider, M.; Claverie, J.; Graillat, C.; McKenna, T. F. J Appl Polym Sci 2002, 84, 1878.
7. Chu, F.; Guillot, J.; Guyot, A. Colloid Polym Sci 1998, 276, 305.
8. Chu, F.; Guyot, A. Colloid Polym Sci 2001, 279, 361.
9. Greenwood, R.; Luckham, P. F.; Gregorg, T. J Colloid Interface Sci 1997, 191, 11.
10. Greenwood, R.; Luckham, P. F.; Gregorg, T. Colloids Surf A 1998, 144, 139.
11. Berend, K.; Richtering, W. Colloids Surf A 1995, 99, 101.
12. Chu, F.; Graillat, C.; Guyot, A. J Appl Polym Sci 1998, 70, 2667.
13. Chu, F.; Guillot, J.; Guyot, A. Polym Adv Technol 1998, 9, 844.
14. Chu, F.; Guillot, J.; Guyot, A. Polym Adv Technol 1998, 9, 851.
15. Schneider, M.; Graillat, C.; Guyot, A.; McKenna, T. F. J Appl Polym Sci 2002, 84, 1897.
16. Schneider, M.; Graillat, C.; Guyot, A.; McKenna, T. F. J Appl Polym Sci 2002, 84, 1916.
17. Schneider, M.; Graillat, C.; Guyot, A.; Betremieux, I.; McKenna, T. F. J Appl Polym Sci 2002, 84, 1935.
18. Ai, Z.; Zhou, Q.; Sun, G.; Zhang, H. Acta Polym Sinica 2005, 7, 754.
19. Eckersley, S. T.; Helmer, B. J. J Coat Technol 1997, 69(864), 97.
20. Winnik, M. A.; Feng, J. J Coat Technol 1996, 68(852), 39.
21. Patel, A. A.; Feng, J.; Winnik, M. A.; Vansco, G. J.; Dittman McBain, C. B. Polymer 1996, 37, 5577.
22. Robeson, L. M.; Berner, R. A. J Polym Sci Part B: Polym Phys 2001, 39, 1093.
23. Lepizzera, S.; Lhommeau, C.; Dilger, G.; Pith, T.; Lambla, M. J Polym Sci Part B: Polym Phys 1997, 2093.